15th Triennial World Congress, Barcelona, Spain

ADAPTIVE SPEED CONTROL WITH FRICTION COMPENSATION FOR SEMI-CURRENT-FED INDUCTION MOTORS*

Kuang-Yow Lian†, Cheng-Yao Hung, Jeih-Jang Liou and Peter Liu

Department of Electrical Engineering
Chung-Yuan Christian University
Chung-Li. 32023 TAIWAN
TEL: 886-3-4563171 ext. 4815
FAX: 886-3-4372194
Email: lian@dec.ee.cycu.edu.tw

Abstract: In this paper, the speed control problem of induction motors is considered based on a *semi-current-fed* model considering the LuGre dynamic friction model. A *double-observer* structure is used to estimate different nonlinear effects of the immeasurable friction state. For the *semi-current-fed* model, either a bounded current-loop control force (stator voltage) and/or a finite integral of current tracking error are assumed which relaxes the traditional strict assumption of an ideal current-loop. In practical experiments, it is assumed that the rotor resistance, torque load, and friction parameters are unknown. *Copyright © 2002 IFAC*

Keywords: Induction motors, friction, adaptive control, observers, speed control

1. INTRODUCTION

The induction motor (IM) driven by current control inverters has high-gain current loops so that the stator currents may be assumed to be the control inputs. The feasibility of frequency, magnitude, and phase control of the stator currents makes the ideal current-fed IM especially suitable for torque control applications (Trzynadlowski, 1994). If the stator currents, instead of stator voltages, are regarded as the control inputs, the dynamic model of the IM can be reduced to a third order model. Based on the reduced-model, the control of IMs become more straightforward. An attractive research problem in current-fed IM is the design of an output feedback algorithm for speed and flux regulation with unknown time-varying rotor resistance and torque load. In the typical control of IMs, a rotor flux observer and a rotor resistance estimator are needed. To cope with the complex bilinear estimation problem, many schemes have been proposed (Marino, *et al.*, 1996).

In this paper, the proposed *semi-current-fed* model is more practical than the typical current-fed model. Here we either assume the current-loop maintains the stator voltage upper bounded and/or that the L_1 norm of the current tracking error is bounded. This approach relaxes the assumption of an ideal current-loop needed in the previous works. We also consider dynamic friction effect presented by a LuGre model (Canudas de Wit, *et al.*, 1995). Hence, the adaptive scheme addressed in (Tan and Kanellakopoulos, 1999) is extended to handle non-uniform parametric variations of the friction force. A nonlinear controller with adaptive friction compensation is proposed to achieve tracking objectives with information of only the rotor speed, stator voltage and current while rotor resistance and torque load are unknown. A set of virtual desired variables (VDV) is utilized and determined in a straightforward manner once considering the principals of vector control — the intention of achieving a well performing current regulator and exact field orientation. To avoid using rotor flux feedback, an auxiliary signal relates the rotor flux error to the measurable signals. The proposed adaptive controller is then

*This work was supported by the National Science Council, R.O.C, under Grant NSC-87-2213-E033-024.
†Correspondance addressee.

proven to achieve asymptotic speed tracking. In addition, flux tracking is achieved under the condition of persistent excitation.

2. PROBLEM FORMULATION

2.1 Dynamical Model of Induction Motors with Considering Friction

The model of a three-phase IM is represented by (Tan and Kanellakopoulos, 1999; Bose, *et al.*, 1986):

$$\begin{aligned} \beta\dot{\mathbf{i}} + \Phi\mathbf{i} + \Theta\boldsymbol{\lambda} &= \tfrac{L_r}{L_m}\mathbf{V}_s & (1)\\ \dot{\boldsymbol{\lambda}} - \Theta\boldsymbol{\lambda} - \tfrac{L_m R_r}{L_r}\mathbf{i} &= 0 & (2)\\ J\dot{\omega} &= T - T_l - F & (3)\\ T &= \tfrac{n_p L_m}{L_r}\mathbf{i}^{\mathrm{T}}\mathbf{J}_2\boldsymbol{\lambda} & (4) \end{aligned}$$

where $\Phi = \frac{L_r R_s}{L_m} + \frac{L_m R_r}{L_r}$, $\Theta = \omega\mathbf{J}_2 - \frac{R_r}{L_r}\mathbf{I}_2$, $\beta = \frac{\sigma L_r}{L_m}$, $\mathbf{i} = [i_{sa}\ i_{sb}]^{\mathrm{T}}$, $\boldsymbol{\lambda} = [\lambda_{ra}\ \lambda_{rb}]^{\mathrm{T}}$, $\mathbf{V}_s = [V_{sa}\ V_{sb}]^{\mathrm{T}}$, $\mathbf{I}_2 = diag\{1, 1\}$, $\mathbf{J}_2 = \begin{bmatrix} 0 & -1 \\ 1 & 0 \end{bmatrix}$. Let (i_{sa}, i_{sb}), $(\lambda_{ra}, \lambda_{rb})$ and ω denote the components of the stator current, rotor flux, and rotor speed, respectively. The (V_{sa}, V_{sb}) denote the stator voltages; R_s, R_r, L_s, L_r and L_m are the stator resistance, rotor resistance, stator inductance, rotor inductance, and mutual inductance, respectively; parameter $\sigma = L_s - L_m^2/L_r$; J, T_l, F are the mechanical inertia, torque load, friction force, respectively; and T is a scalar function representing the electromechanical coupling torque expressed as: $T = \frac{n_p L_m}{L_r}(\lambda_{ra} i_{sb} - \lambda_{rb} i_{sa})$, where n_p denotes one and a half the pole pair number. Furthermore, the friction force F is modeled by the LuGre friction model (Canudas de Wit, *et al.*, 1995) with friction force variations:

$$\begin{aligned} \tfrac{dz}{dt} &= \omega - \tfrac{|\omega|}{g(\omega)}z & (5)\\ F &= \sigma_0 z + \sigma_1\tfrac{dz}{dt} + \sigma_2\omega, & (6) \end{aligned}$$

where z is the friction state that physically stands for the average deflection of the bristles between two contact surfaces. The friction force parameters σ_0, σ_1, σ_2 can be physically explained as the stiffness of bristles, damping coefficient, and viscous coefficient, respectively. In our design we assume that these three parameters are unknown positive constants. A parameterization of $g(\omega) = F_C + (F_S - F_C)\, e^{-\left(\frac{\omega}{\omega_s}\right)^2}$ has been proposed to describe the Stribeck effect (Canudas de Wit, *et al.*, 1995), where F_C is the Coulomb friction value, F_S is the value of the stiction force, and ω_s is the Stribeck velocity.

2.2 Problem Formulation

In current-fed IM systems, high-gain PI current loops are imposed to regulate the stator currents. The concise block diagram of a practical current-fed IM system is shown in Fig. 1. The block diagram illustrates that the stator currents (i_{sa}, i_{sb}) are forced to track the reference signals (i_{sa}^*, i_{sb}^*) by virtue of the PI control input defined as follows:

$$\begin{aligned} V_{sa} &= -K_{ap}\widetilde{i}_{sa} - K_{ai}\textstyle\int_0^t \widetilde{i}_{sa}dt & (7)\\ V_{sb} &= -K_{bp}\widetilde{i}_{sb} - K_{bi}\textstyle\int_0^t \widetilde{i}_{sb}dt & (8) \end{aligned}$$

where $\widetilde{i}_{sa} = i_{sa} - i_{sa}^*$, $\widetilde{i}_{sb} = i_{sb} - i_{sb}^*$, and the positive gains K_{ap}, K_{ai}, K_{bp}, K_{bi} are properly chosen such that the current loop has satisfactory performance. Therefore, the dynamics of the stator currents (1) can be neglected and the reference values of the stator are considered as the control inputs. In other words, we replace (i_{sa}, i_{sb}) with (i_{sa}^*, i_{sb}^*). Finally, the reduced-order model of the IM is expressed by (2) and (3). However, the assumption of an ideal current loop control in practical situations is not easily satisfied. This is due to current loop uncertainties and saturation of high gain control. To cope with this problem, a semi-current-fed concept is stated in the following assumptions:

A.1: By proper choice of PI gains in (7) and (8), the current loop performs well such that $\mathbf{V}_s$ is bounded, i.e., $\mathbf{V}_s \in L_\infty$.

Since (7) and (8) is viewed here as a stable filter driven by $\mathbf{V}_s$, we have $\widetilde{i}_{sa}, \widetilde{i}_{sb} \in L_\infty$ according to A.1. A stronger assumption is made as follows:

A.1': In addition to A.1, the current tracking errors are assumed to be a finite integrable function, i.e., $\widetilde{i}_{sa}, \widetilde{i}_{sb} \in L_\infty \cap L_1$.

Under the sense of A.1 or A.1', we call this current controlled IM as a *semi-current-fed* IM. This terminology arises from the fact that A.1 and A.1' relaxes the assumption $i_{sa} = i_{sa}^*$, $i_{sb} = i_{sb}^*$, which has been needed in typical current-fed IM control. Therefore the speed control design based on a semi-current-fed concept is a step closer to practical situations. Before the controller synthesis, some other assumptions are given:

A.2 The voltages and currents of stator, along with the velocity of rotor are considered to be measurable.

A.3 Moment of inertia J and the load torque T_l are unknown constant.

A.4 The parameters, L_m, L_r, R_s, are known constants whereas R_r is unknown.

A.5 The desired speed ω_d is a smooth and

bounded function.

3. ADAPTIVE SPEED CONTROL DESIGN

3.1 Mechanical Loop Control and VDV-Synthesis

First, let us consider the mechanical dynamics (3). The speed tracking error $\tilde{\omega} \equiv \omega - \omega_d$. Therefore, (3) is rewritten in terms of $\tilde{\omega}$ as follows:

$$\begin{aligned} & J\dot{\tilde{\omega}} + B\tilde{\omega} \\ = \; & T - T_d + T_d - T_l - J\dot{\omega}_d \\ & -B\omega_d - \sigma_0 z + \sigma_1 \tfrac{|\omega|}{g(\omega)} z \end{aligned} \tag{9}$$

where $B \equiv \sigma_1 + \sigma_2 > 0$. As we know, the friction state z is not measurable. In order to cope with different nonlinearities of z that are present in the system dynamics, we employ two nonlinear observers to estimate the immeasurable state z and replace z with its estimates $\widehat{z}_0$ and $\widehat{z}_1$, of which the dynamics are given by

$$\tfrac{d\widehat{z}_0}{dt} = \omega - \tfrac{|\omega|}{g(\omega)}\widehat{z}_0 + \iota_0,\; \tfrac{d\widehat{z}_1}{dt} = \omega - \tfrac{|\omega|}{g(\omega)}\widehat{z}_1 + \iota_1 \tag{10}$$

where ι_0, ι_1 are compensation terms that are yet to be determined. The estimation error $\widetilde{z}_0 = z - \widehat{z}_0$ and $\widetilde{z}_1 = z - \widehat{z}_1$. In light of this, (9) is further written as:

$$\begin{aligned} & J\dot{\tilde{\omega}} + (B + k_\omega)\,\tilde{\omega} \\ = \; & T - T_d + T_d - \mathbf{Y}\boldsymbol{\theta} + k_\omega\tilde{\omega} \\ & -\sigma_0\left(\widetilde{z}_0 + \widehat{z}_0\right) + \sigma_1 \tfrac{|\omega|}{g(\omega)}\left(\widetilde{z}_1 + \widehat{z}_1\right) \end{aligned} \tag{11}$$

where T_d denotes the desired torque which produces the desired speed; k_ω is a adjustable damping ratio; $\mathbf{Y} = [1 \;\; \dot{\omega}_d \;\; \omega_d]$ is a regression matrix; and the parameter vector $\boldsymbol{\theta} \equiv [T_l \;\; J \;\; B]^{\mathrm{T}}$. The damping term $k_\omega\tilde{\omega}$ plays a dominant role on the transient response for speed tracking. For speed tracking control, the desired torque is naturally defined to be

$$T_d = \mathbf{Y}\widehat{\boldsymbol{\theta}} - k_\omega\tilde{\omega} + \widehat{\sigma}_0\widehat{z}_0 - \tfrac{|\omega|}{g(\omega)}\widehat{\sigma}_1\widehat{z}_1 \tag{12}$$

where $\widehat{\boldsymbol{\theta}}$ is the estimated vector of $\boldsymbol{\theta}$. Therefore the following error dynamics is obtained:

$$\begin{aligned} & J\dot{\tilde{\omega}} + (B + k_\omega)\,\tilde{\omega} \\ = \; & T - T_d - \mathbf{Y}\widetilde{\boldsymbol{\theta}} - \sigma_0\widetilde{z}_0 - \widetilde{\sigma}_0\widehat{z}_0 \\ & +\sigma_1 \tfrac{|\omega|}{g(\omega)}\widetilde{z}_1 + \widetilde{\sigma}_1 \tfrac{|\omega|}{g(\omega)}\widehat{z}_1 \end{aligned} \tag{13}$$

with the estimation error $\widetilde{\boldsymbol{\theta}} \equiv \boldsymbol{\theta} - \widehat{\boldsymbol{\theta}}$. If the update laws for $\widehat{\boldsymbol{\theta}}$, $\widehat{\sigma}_0$, and $\widehat{\sigma}_1$ are properly chosen and $(T - T_d)$, $\widetilde{z}_0$, and $\widetilde{z}_1$ are driven to zero, the rotor speed will converge to the desired value at a desired rate based on a suitably chosen k_ω. To this end, the speed tracking control problem has been reformulated into the torque tracking problem. In other words, the remainder of the control design is to generate a torque T to track the desired torque T_d while all internal signals are maintained bounded. Consider the cascaded subsystems (1) and (2), the vector control problem is to design a desired current $\mathbf{i}^*$ and flux $\boldsymbol{\lambda}_d$ independently such that the electrical subsystem can generate the desired torque T_d, where $\boldsymbol{\lambda}_d$ is a virtual desired variable for $\boldsymbol{\lambda}$ to achieve. From the above and torque equation (4), we synthesize T_d by

$$T_d = \tfrac{n_p L_m}{L_r}\mathbf{i}^{*\mathrm{T}}\mathbf{J}_2\boldsymbol{\lambda}_d \tag{14}$$

Once $\mathbf{i}$ and $\boldsymbol{\lambda}$ converge to $\mathbf{i}^*$ and $\boldsymbol{\lambda}_d$ respectively, then T converges to T_d. This can be a way to design $\mathbf{V}_s$ for a full model. In contrast, based on the semi-current-fed concept, the convergence of $\mathbf{i}$ to $\mathbf{i}^*$ depends on whether the current loop controller satisfies the assumptions A.1 or A.1'. Consequently, the torque tracking is reformulated into designing $\mathbf{i}^*$ and $\boldsymbol{\lambda}_d$ such that $\boldsymbol{\lambda} \to \boldsymbol{\lambda}_d$ while satisfying (14). In light of vector control analysis, we impose some conditions on the virtual desired variables $\mathbf{i}^*$ and $\boldsymbol{\lambda}_d$. First, we note that the optimal torque will be obtained by setting the magnitude of magnetic flux to be a constant value. Therefore to achieve this property, we let $\|\boldsymbol{\lambda}_d\| = c$, where c is an given constant. This further implies that the virtual desired flux in the stator frame is $\boldsymbol{\lambda}_d = \left(c\cos(\rho) \;\; c\sin(\rho)\right)$, where $\rho(t)$ denotes the angle between the stator frame and excitation frame which is to be determined later. In light of the above, $\boldsymbol{\lambda}_d$ and $\mathbf{i}^*$ are constrained by the following conditions: **C.1** $\boldsymbol{\lambda}_d$ is kept constant by letting $\|\boldsymbol{\lambda}_d\| = c$; **C.2** $\boldsymbol{\lambda}_d$ and $\mathbf{i}^*$ satisfy (14). As a result, the control objective is to design $\mathbf{i}^*$ such that $\boldsymbol{\lambda} \to \boldsymbol{\lambda}_d$, where $\boldsymbol{\lambda}_d$ is constrained by C.1 and C.2.

3.2 Realization of VDV-Synthesis

Since the rotor flux is not measurable, we omit the use of flux sensors and reconstruct the flux signals without using an observer. From (1) and (2), we have:

$$\beta\dot{\mathbf{i}} + \dot{\boldsymbol{\lambda}} = \dot{\boldsymbol{\eta}} \tag{15}$$

where $\dot{\boldsymbol{\eta}} = -\tfrac{L_r R_s}{L_m}\mathbf{i} + \tfrac{L_r}{L_m}\mathbf{V}_s$ is a first order filter. Integrating (15), the flux signals

$$\boldsymbol{\lambda} = \boldsymbol{\eta} - \beta\mathbf{i} + \mathbf{A} \tag{16}$$

where $\mathbf{A}$ is an unknown integration constant vector dependent on initial conditions. In virtue of (16), the reconstructed flux signals $\widehat{\boldsymbol{\lambda}} = \boldsymbol{\eta} - \beta\mathbf{i} + \widehat{\mathbf{A}}$, where $\widehat{\mathbf{A}}$ is an estimated signal of $\mathbf{A}$ and is to be determined by the adaptive mechanism. The VDV-synthesis algorithm is given in the following:

Step 1 First, change the original flux tracking into the tracking of reconstructed flux $\widehat{\boldsymbol{\lambda}}$ to $\boldsymbol{\lambda}_d$.

Define the tracking error of reconstructed flux, error of estimated rotor resistance, and error of estimated integration constant, respectively, as $\widetilde{\boldsymbol{\lambda}} = \widehat{\boldsymbol{\lambda}} - \boldsymbol{\lambda}_d$, $\widetilde{R}_r = R_r - \widehat{R}_r$, and $\widetilde{\mathbf{A}} = \mathbf{A} - \widehat{\mathbf{A}}$, where $\widehat{R}_r$ is the estimated rotor resistance. From (2), we obtain

$$\begin{aligned}\dot{\widetilde{\boldsymbol{\lambda}}} &= \dot{\boldsymbol{\lambda}} + \dot{\widehat{\mathbf{A}}} - \dot{\boldsymbol{\lambda}}_d \\ &= \left(\omega \mathbf{J}_2 - \frac{R_r}{L_r}\mathbf{I}_2 - \frac{L_m R_r}{L_r} k_\lambda\right)\widetilde{\boldsymbol{\lambda}} + \widetilde{R}_r \boldsymbol{\phi}_r \\ &\quad + \omega \mathbf{J}_2 \widetilde{\mathbf{A}} - \widetilde{\mathbf{B}} + \frac{L_m}{L_r} R_r \widetilde{\mathbf{i}} + \boldsymbol{\xi}_\lambda - \boldsymbol{\varsigma} \end{aligned} \quad (17)$$

where $\widetilde{\mathbf{i}} \equiv \mathbf{i} - \mathbf{i}^*$; $\widetilde{\mathbf{B}} \equiv \mathbf{B} - \widehat{\mathbf{B}}$, where $\widehat{\mathbf{B}}$ is the estimated signal of $\mathbf{B} \equiv \frac{R_r}{L_r}\mathbf{A}$; $k_\lambda > 0$; $\boldsymbol{\varsigma}$ is an auxiliary signal determined later; and $\boldsymbol{\xi}_\lambda = (\omega \mathbf{J}_2 - \frac{\widehat{R}_r}{L_r}\mathbf{I}_2)\boldsymbol{\lambda}_d + \frac{L_m \widehat{R}_r}{L_r} k_\lambda \widetilde{\boldsymbol{\lambda}} - \widehat{\mathbf{B}} + \frac{\widehat{R}_r}{L_r}\widehat{\mathbf{A}} + \frac{L_m}{L_r}\widehat{R}_r \mathbf{i}^* + \dot{\widehat{\mathbf{A}}} - \dot{\boldsymbol{\lambda}}_d + \boldsymbol{\varsigma}$, $\boldsymbol{\phi}_r = \frac{L_m}{L_r}\mathbf{i}^* - \frac{1}{L_r}\boldsymbol{\lambda}_d + \frac{1}{L_r}\widehat{\mathbf{A}} + \frac{L_m}{L_r} k_\lambda \widetilde{\boldsymbol{\lambda}}$. Since $\boldsymbol{\xi}_\lambda$ is a perturbation term in (17), set $\boldsymbol{\xi}_\lambda = 0$ to determine $\mathbf{i}^*$ and ρ. From definition of $\boldsymbol{\lambda}_d$, we obtain

$$\begin{aligned}\mathbf{i}^* &= \frac{L_r}{L_m \widehat{R}_r}\left((\dot{\rho} - \omega)\mathbf{J}_2 \boldsymbol{\lambda}_d + \widehat{\mathbf{B}} - \dot{\widehat{\mathbf{A}}} - \boldsymbol{\varsigma}\right) \\ &\quad - \frac{1}{L_m}\left(\widehat{\mathbf{A}} - \boldsymbol{\lambda}_d\right) - k_\lambda \widetilde{\boldsymbol{\lambda}} \end{aligned} \quad (18)$$

where the relation $\dot{\boldsymbol{\lambda}}_d = \dot{\rho}\mathbf{J}_2 \boldsymbol{\lambda}_d$ (c.f., C.1) has been used.

Step 2 Substitute (18) into (14) (i.e., satisfying C.2). The result of the substitution along with C.1 is used to determine the angle $\rho(t)$ where

$$\begin{aligned}\dot{\rho} &= \omega + \frac{1}{c^2}\left(\widehat{R}_r\left(\frac{T_d}{n_p} + \frac{L_m}{L_r} k_\lambda \widetilde{\boldsymbol{\lambda}}^{\mathrm{T}} \mathbf{J}_2 \boldsymbol{\lambda}_d \right.\right. \\ &\quad \left.\left. + \frac{1}{L_r}\widehat{\mathbf{A}}^{\mathrm{T}} \mathbf{J}_2 \boldsymbol{\lambda}_d\right) + \left(\dot{\widehat{\mathbf{A}}} + \boldsymbol{\varsigma} - \widehat{\mathbf{B}}\right)^{\mathrm{T}} \mathbf{J}_2 \boldsymbol{\lambda}_d\right) \end{aligned} \quad (19)$$

Therefore $\mathbf{i}^*$ can be rewritten in terms of T_d :

$$\begin{aligned}\mathbf{i}^* &= \frac{1}{L_m}\left(\mathbf{I}_2 + \frac{1}{c^2}\psi \mathbf{J}_2\right)\boldsymbol{\lambda}_d \\ &\quad + \frac{L_r}{L_m \widehat{R}_r}\left(\widehat{\mathbf{B}} - \dot{\widehat{\mathbf{A}}} - \boldsymbol{\varsigma}\right) - k_\lambda \widetilde{\boldsymbol{\lambda}} - \frac{1}{L_m}\widehat{\mathbf{A}}, \end{aligned} \quad (20)$$

where $\psi = (L_m k_\lambda \widetilde{\boldsymbol{\lambda}} + \widehat{\mathbf{A}})^{\mathrm{T}} \mathbf{J}_2 \boldsymbol{\lambda}_d + L_r(\frac{T_d}{n_p} + \frac{1}{\widehat{R}_r}(\dot{\widehat{\mathbf{A}}} + \boldsymbol{\varsigma} - \widehat{\mathbf{B}})^{\mathrm{T}} \mathbf{J}_2 \boldsymbol{\lambda}_d)$.

3.3 Adaptive Mechanism

Based on the control law (20), the error dynamics (13) and (17) are further expressed as

$$\begin{aligned} & J\dot{\widetilde{\omega}} + (B + k_\omega)\widetilde{\omega} \\ &= \frac{L_m n_p}{L_r}\left(\mathbf{i}^{\mathrm{T}} \mathbf{J}_2 \widetilde{\boldsymbol{\lambda}} + \mathbf{i}^{\mathrm{T}} \mathbf{J}_2 \widetilde{\mathbf{A}} + \widetilde{\mathbf{i}}^{\mathrm{T}} \mathbf{J}_2 \boldsymbol{\lambda}_d\right) \\ &\quad - \mathbf{Y}\widetilde{\boldsymbol{\theta}} - \sigma_0 \widetilde{z}_0 - \widetilde{\sigma}_0 \widehat{z}_0 + \sigma_1 \frac{|\omega|}{g(\omega)}\widetilde{z}_1 + \widetilde{\sigma}_1 \frac{|\omega|}{g(\omega)}\widehat{z}_1 \end{aligned} \quad (21)$$

$$\begin{aligned}\dot{\widetilde{\boldsymbol{\lambda}}} &= \left(\omega \mathbf{J}_2 - \frac{R_r}{L_r}\mathbf{I}_2 - \frac{L_m R_r}{L_r} k_\lambda \mathbf{I}_2\right)\widetilde{\boldsymbol{\lambda}} + \widetilde{R}_r \boldsymbol{\phi}_r \\ &\quad + \omega \mathbf{J}_2 \widetilde{\mathbf{A}} - \widetilde{\mathbf{B}} + \frac{L_m}{L_r} R_r \widetilde{\mathbf{i}} - \boldsymbol{\varsigma} \end{aligned} \quad (22)$$

where (4) and (14) have been used. If the current error $(\mathbf{i} - \mathbf{i}^*)$ is the input of the PI current controller (7) and (8), the semi-current-fed concept is achieved. We now show that the tracking errors $\widetilde{\omega}$ and $\widetilde{\boldsymbol{\lambda}}$ are convergent once update laws for $\widehat{R}_r$, $\widehat{\boldsymbol{\theta}}$, $\widehat{\mathbf{A}}$, $\widehat{\mathbf{B}}$, $\widehat{\sigma}_0$, and $\widehat{\sigma}_1$ are suitably chosen. Consider a Lyapunov function candidate

$$\begin{aligned}V &= \frac{1}{2}\alpha J \widetilde{\omega}^2 + \frac{1}{2}\alpha \widetilde{\boldsymbol{\theta}}^{\mathrm{T}} \boldsymbol{\Gamma}_4^{-1} \widetilde{\boldsymbol{\theta}} + \frac{1}{2}\left(\widetilde{\boldsymbol{\lambda}}^{\mathrm{T}} \widetilde{\boldsymbol{\lambda}} + \gamma_1^{-1}\widetilde{R}_r^2 \right. \\ &\quad + \widetilde{\mathbf{A}}^{\mathrm{T}} \boldsymbol{\Gamma}_2^{-1} \widetilde{\mathbf{A}} + \widetilde{\mathbf{B}}^{\mathrm{T}} \boldsymbol{\Gamma}_3^{-1} \widetilde{\mathbf{B}} + \gamma_5^{-1}\widetilde{\sigma}_0^2 \\ &\quad \left. + \gamma_6^{-1}\widetilde{\sigma}_1^2\right) + \frac{1}{2}\sigma_0 \widetilde{z}_0^2 + \frac{1}{2}\sigma_1 \widetilde{z}_1^2 \end{aligned} \quad (23)$$

where α is an arbitrary positive constant; and γ_1, $\boldsymbol{\Gamma}_2 = \boldsymbol{\Gamma}_2^{\mathrm{T}}$, $\boldsymbol{\Gamma}_3 = \boldsymbol{\Gamma}_3^{\mathrm{T}}$, $\boldsymbol{\Gamma}_4 = \boldsymbol{\Gamma}_4^{\mathrm{T}}$, γ_5, γ_6, are positive definite adaptation gains. The time derivative of (23) is $\dot{V} = \alpha J \dot{\widetilde{\omega}}\widetilde{\omega} + \alpha \widetilde{\boldsymbol{\theta}}^{\mathrm{T}} \boldsymbol{\Gamma}_4^{-1} \dot{\widetilde{\boldsymbol{\theta}}} + \widetilde{\boldsymbol{\lambda}}^{\mathrm{T}} \dot{\widetilde{\boldsymbol{\lambda}}} + \gamma_1^{-1}\widetilde{R}_r \dot{\widetilde{R}}_r + \widetilde{\mathbf{A}}^{\mathrm{T}} \boldsymbol{\Gamma}_2^{-1} \dot{\widetilde{\mathbf{A}}} + \widetilde{\mathbf{B}}^{\mathrm{T}} \boldsymbol{\Gamma}_3^{-1} \dot{\widetilde{\mathbf{B}}} + \sigma_0 \widetilde{z}_0 \dot{\widetilde{z}}_0 + \sigma_1 \widetilde{z}_1 \dot{\widetilde{z}}_1 + \gamma_5^{-1}\widetilde{\sigma}_0 \dot{\widetilde{\sigma}}_0 + \gamma_6^{-1}\widetilde{\sigma}_1 \dot{\widetilde{\sigma}}_1$. To render $\dot{V} < 0$, the update law of $\widehat{R}_r$ is chosen as:

$$\dot{\widehat{R}}_r = \begin{cases} 0, & \text{if } \widehat{R}_r = R_0 \text{ and } \widetilde{\boldsymbol{\lambda}}^{\mathrm{T}} \boldsymbol{\phi}_r < 0 \\ \gamma_1 \widetilde{\boldsymbol{\lambda}}^{\mathrm{T}} \boldsymbol{\phi}_r, & \text{otherwise} \end{cases} \quad (24)$$

where R_0 denotes a lower bound of the unknown rotor resistance R_r. The update law for $\widehat{R}_r$ satisfies $\widetilde{R}_r(\gamma_1^{-1}\dot{\widetilde{R}}_r + \widetilde{\boldsymbol{\lambda}}^{\mathrm{T}} \boldsymbol{\phi}_r) = -\widetilde{R}_r \gamma_1^{-1}(\dot{\widehat{R}}_r - \gamma_1 \widetilde{\boldsymbol{\lambda}}^{\mathrm{T}} \boldsymbol{\phi}_r) \leq 0$, since $R_r > R_0$. The other update laws for $\widehat{\mathbf{A}}$, $\widehat{\mathbf{B}}$ and $\widehat{\boldsymbol{\theta}}$ are

$$\dot{\widehat{\mathbf{A}}} = \boldsymbol{\Gamma}_2\left(\frac{\alpha L_m n_p}{L_r}\widetilde{\omega}\mathbf{J}_2^{\mathrm{T}}\mathbf{i} + \omega \mathbf{J}_2^{\mathrm{T}}\widetilde{\boldsymbol{\lambda}}\right) \quad (25)$$

$$\dot{\widehat{\mathbf{B}}} = -\boldsymbol{\Gamma}_3 \widetilde{\boldsymbol{\lambda}}, \dot{\widehat{\boldsymbol{\theta}}} = -\widetilde{\omega}\boldsymbol{\Gamma}_4 \mathbf{Y}^{\mathrm{T}} \quad (26)$$

$$\dot{\widehat{\sigma}}_0 = -\gamma_5 \alpha \widetilde{\omega}\widehat{z}_0, \dot{\widehat{\sigma}}_1 = \gamma_6 \alpha \widetilde{\omega}\frac{|\omega|}{g(\omega)}\widehat{z}_1 \quad (27)$$

Accordingly the observer compensation terms are defined by:

$$\iota_0 = -\alpha\widetilde{\omega}, \iota_1 = \frac{|\omega|}{g(\omega)}\alpha\widetilde{\omega} \quad (28)$$

where the auxiliary signal $\boldsymbol{\varsigma}$ is given as

$$\boldsymbol{\varsigma} = \frac{\alpha L_m n_p}{L_r}\widetilde{\omega}\mathbf{J}_2^{\mathrm{T}}\mathbf{i} \quad (29)$$

As a result, we arrive with the following inequality

$$\begin{aligned}\dot{V} &= -\alpha(B + k_\omega)\widetilde{\omega}^2 - \frac{R_r}{L_r}(1 + L_m k_\lambda)\widetilde{\boldsymbol{\lambda}}^{\mathrm{T}}\widetilde{\boldsymbol{\lambda}} \\ &\quad + \frac{L_m}{L_r}\widetilde{\mathbf{i}}^{\mathrm{T}}\begin{bmatrix} \alpha n_p \mathbf{J}_2 \boldsymbol{\lambda}_d & R_r \mathbf{I}_2 \end{bmatrix}\begin{bmatrix} \widetilde{\omega} \\ \widetilde{\boldsymbol{\lambda}} \end{bmatrix} \\ &\quad - \sigma_0 \frac{|\omega|}{g(\omega)}\widetilde{z}_0^2 - \sigma_1 \frac{|\omega|}{g(\omega)}\widetilde{z}_1^2 \end{aligned} \quad (30)$$

Theorem: Consider a semi-current-fed IM of which the friction force variation is characterized

by the friction model in (5), (6). The control law (20) is composed of the dual observer structure (10), (28) for the friction force, the desired torque T_d in (12), the auxiliary signal $\boldsymbol{\varsigma}$ in (29), and the parameter update laws (25)$\sim$(27). If the control gains k_ω, k_λ, c and α are suitably chosen, the closed-loop control system has the following properties:

(a) If A.1$\sim$A.5 are satisfied, all signals in the closed-loop system are bounded. Moreover, the tracking errors $\tilde{\omega}$ and $\widetilde{\boldsymbol{\lambda}}$ with respect to the current error $\widetilde{\mathbf{i}}$ is finite-gain L_2 stable, i.e., $\int_0^t \|\mathbf{h}(\tau)\|^2 d\tau \leq \epsilon_1 + \epsilon_2 \int_0^t \left\|\widetilde{\mathbf{i}}(\tau)\right\|^2 d\tau$ for $\mathbf{h} = [\tilde{\omega}\ \widetilde{\boldsymbol{\lambda}}^{\mathrm{T}}]^{\mathrm{T}}$ and some positive constants ϵ_1 and ϵ_2.

(b) If A.1', A.2$\sim$A.5 are satisfied, then the tracking errors $\tilde{\omega}$ and $\widetilde{\boldsymbol{\lambda}}$ asymptotically converge to zero as $t \to \infty$.

Proof. The proof is omitted due to lack of space. ■

Here we emphasize that in our proposed methodology, no PE condition is needed. Now we analyze the rotor flux tracking error $(\boldsymbol{\lambda} - \boldsymbol{\lambda}_d)$ under assumption that the projection of update law (24) does not occur. In other words, $\dot{\widehat{R}}_r = \gamma_1 \widetilde{\boldsymbol{\lambda}}^{\mathrm{T}} \boldsymbol{\phi}_r$. The overall error dynamics (21) and (22) is rewritten as

$$\boldsymbol{\Lambda}\dot{\mathbf{X}} = \mathbf{P}(t)\,\mathbf{X} + \mathbf{S}(t)\,\widetilde{\mathbf{i}} \tag{31}$$

where $\mathbf{X} = [\tilde{\omega}\ \widetilde{\boldsymbol{\lambda}}^{\mathrm{T}}\ \widetilde{z}_0\ \widetilde{z}_1\ \widetilde{R}_r\ \widetilde{\mathbf{A}}^{\mathrm{T}}\ \widetilde{\mathbf{B}}^{\mathrm{T}}\ \widetilde{\boldsymbol{\theta}}^{\mathrm{T}}\ \widetilde{\sigma}_0\ \widetilde{\sigma}_1]^{\mathrm{T}}$, $\boldsymbol{\Lambda} = \textit{block-diag}\{\alpha J,\ \mathbf{I}_4,\ \mathbf{I}_5,\ \alpha\mathbf{I}_3,\ \mathbf{I}_2\}$, and $\boldsymbol{\Gamma} = \textit{block-diag}\{\gamma_1, \boldsymbol{\Gamma}_2, \boldsymbol{\Gamma}_3, \boldsymbol{\Gamma}_4, \gamma_5, \gamma_6\}$.

$$\mathbf{P} = \left[\begin{array}{cccc|c} \mathbf{P}_{11} & \mathbf{P}_{12} & \mathbf{P}_{13} & \mathbf{P}_{13} & \\ \mathbf{P}_{21} & \mathbf{P}_{22} & \mathbf{P}_{23} & \mathbf{P}_{24} & \mathbf{w}^{\mathrm{T}} \\ \mathbf{P}_{31} & \mathbf{P}_{32} & \mathbf{P}_{33} & \mathbf{P}_{34} & \\ \mathbf{P}_{41} & \mathbf{P}_{42} & \mathbf{P}_{43} & \mathbf{P}_{44} & \\ \hline -\boldsymbol{\Gamma}\mathbf{W} & & & & 0 \end{array}\right],$$

$$\mathbf{S} = \left[\begin{array}{c} \frac{\alpha L_m n_p}{L_r}\boldsymbol{\lambda}_d^{\mathrm{T}}\mathbf{J}_2^{\mathrm{T}} \\ \frac{L_m R_r}{L_r}\mathbf{I}_2 \\ 0 \end{array}\right],$$

$$\mathbf{W}^{\mathrm{T}} = \left[\begin{array}{cccccc} \mathbf{W}_{11} & \mathbf{W}_{12} & \mathbf{W}_{13} & \mathbf{W}_{14} & \mathbf{W}_{15} & \mathbf{W}_{16} \\ \mathbf{W}_{21} & \mathbf{W}_{22} & \mathbf{W}_{23} & \mathbf{W}_{24} & \mathbf{W}_{25} & \mathbf{W}_{26} \end{array}\right],$$

where $\mathbf{P}_{11} = -\alpha(B + k_\omega)$, $\mathbf{P}_{21} = -\frac{\alpha L_m n_p}{L_r}\mathbf{J}_2^{\mathrm{T}}\mathbf{i}$, $\mathbf{P}_{31} = \alpha$, $\mathbf{P}_{41} = -\frac{|\omega|}{g(\omega)}\alpha$, $\mathbf{P}_{12} = \frac{\alpha L_m n_p}{L_r}\mathbf{i}^{\mathrm{T}}\mathbf{J}_2$, $\mathbf{P}_{22} = \left(\omega\mathbf{J}_2 - \frac{R_r}{L_r}(1 + L_m k_\lambda)\right)\mathbf{I}_2$, $\mathbf{P}_{32} = 0$, $\mathbf{P}_{42} = 0$, $\mathbf{P}_{13} = -\alpha\sigma_0$, $\mathbf{P}_{23} = 0$, $\mathbf{P}_{33} = -\frac{|\omega|}{g(\omega)}$, $\mathbf{P}_{43} = 0$, $\mathbf{P}_{42} = 0$, $\mathbf{P}_{14} = \frac{|\omega|}{g(\omega)}\alpha\sigma_1$, $\mathbf{P}_{24} = 0$, $\mathbf{P}_{34} = 0$, $\mathbf{P}_{44} = -\frac{|\omega|}{g(\omega)}$, and $\mathbf{W}_{11} = 0$, $\mathbf{W}_{21} = \boldsymbol{\phi}_r$, $\mathbf{W}_{12} = \frac{\alpha L_m n_p}{L_r}\mathbf{i}^{\mathrm{T}}\mathbf{J}_2$, $\mathbf{W}_{22} = \omega\mathbf{J}_2$, $\mathbf{W}_{13} = 0$, $\mathbf{W}_{23} = -\mathbf{I}_2$, $\mathbf{W}_{14} = -\alpha\mathbf{Y}$, $\mathbf{W}_{24} = 0$, $\mathbf{W}_{15} = -\alpha\widehat{z}_0$, $\mathbf{W}_{25} = 0$, $\mathbf{W}_{16} = \frac{|\omega|}{g(\omega)}\alpha\widehat{z}_1$, $\mathbf{W}_{26} = 0$.

Corollary Consider a semi-current-fed IM, where A.1' is sustained. If the matrix $\mathbf{W}(t)$ satisfies the persistent excitation condition, that is, there exist two positive constants ν and μ such that

$$\int_t^{t+\nu} \mathbf{W}(\tau)\,\mathbf{W}^{\mathrm{T}}(\tau)\,d\tau \geq \mu\mathbf{I} > 0,\ \forall\ t \geq 0, \tag{32}$$

the equilibrium point $\mathbf{X} = 0$ of system (31) is uniformly asymptotically stable. Furthermore, asymptotic flux tracking will be achieved, that is, $\lim_{t\to\infty}(\boldsymbol{\lambda} - \boldsymbol{\lambda}_d) = 0$.

Proof. The proof is omitted due to lack of space. ■

From above, optimal torque will be sustained if PE is satisfied.

4. EXPERIMENTAL RESULTS

The experimental setup is shown in Fig. 2. The IM parameters expressed in per unit values: rated output power = 0.4 kw; pole pair number = 3; rated V_s = 120 V; rated I_s = 3.4 A; rated T = 2.54; rated ω = 1500 rpm; nominal value of J = 0.001 N-m-s; R_s = 2.85Ω; R_r = 4.0Ω; L_s = 0.19667 H; L_r = 0.19667 H; L_m = 0.1886 H. We first consider speed tracking of $\omega_d = 30\sin 2\pi t$ rad/sec. The control parameters are chosen as: $k_p = -310$, $k_i = -350$, $k_\omega = 1.5$, $k_\lambda = 0.2$ and $\alpha = 0.055$. Update gains are set as $\boldsymbol{\Gamma}_1 = 5.5$, $\boldsymbol{\Gamma}_2 = \textit{diag}\{0.8, 0.8\}$, $\boldsymbol{\Gamma}_3 = \textit{diag}\{0.2, 0.2\}$, $\boldsymbol{\Gamma}_4 = \textit{diag}\{0.1, 6e^{-7}, 0.0007\}$. When the friction compensation is activated, the update gains for the compensation are set as: $\boldsymbol{\Gamma}_4 = \textit{diag}\{0.1, 6e^{-7}, 0.025\}$, $\boldsymbol{\Gamma}_5 = 2$, $\boldsymbol{\Gamma}_6 = 0.82$. The reference signal and speed response with friction force is shown in Fig. 3(a), and with friction compensation is shown in Fig. 3(b). For the case with friction compensation, the response for the speed tracking error is shown in Fig 3(c); the double-observer estimation error $\widetilde{z}_0$, $\widetilde{z}_1$ are shown in Fig. 3(d) and Fig. 3(e), respectively; the input voltage and current for one phase are shown in Fig. 3(f) and Fig. 3(g) respectively; and estimated $\widehat{R}_r$ is shown in Fig. 3(h). Secondly consider speed regulation of ω_d = 30 rad/sec. The control parameters are chosen as: $k_p = -250$, $k_i = -350$, $k_\omega = 1.5$, $k_\lambda = 0.2$ and $\alpha = 0.055$. Update gains are set as $\boldsymbol{\Gamma}_1 = 3.5$, $\boldsymbol{\Gamma}_2 = \textit{diag}\{0.8, 0.8\}$, $\boldsymbol{\Gamma}_3 = \textit{diag}\{0.2, 0.2\}$, $\boldsymbol{\Gamma}_4 = \textit{diag}\{0.1, 6e^{-7}, 0.0046\}$. When the friction compensation is activated, the update gains for the compensation are set as: $\boldsymbol{\Gamma}_4 = \textit{diag}\{0.1, 6e^{-7}, 0.0022\}$, $\boldsymbol{\Gamma}_5 = 10$, $\boldsymbol{\Gamma}_6 = 0.82$. The reference signal and speed response with friction force is shown in Fig. 4(a), and with

friction compensation is shown in Fig. 4(b). The speed tracking error for (b) is shown in Fig 4(c).

5. CONCLUSIONS

In this paper, we consider the speed tracking control with friction compensation for an IM. The IM is modeled by a *semi-current-fed* model whereas the frictional force is by a LuGre dynamic model. From the experimental results, we can see that when considering friction compensation, the performance is greatly improved. Results with smaller overshoot, fasten transient behavior, and nearly zero steady-state error are obtained.

REFERENCES

Trzynadlowski, A.M. (1994). *The Field Orientation Principle in Control of Induction Motors.* Boston: Kluwer Academic Publishers.

Marino, R., S. Peresada, and P. Tomei, (1996). Output feedback control of current-fed induction motor with unknown rotor resistance. *IEEE Trans. Control System Technology*, **vol. 4**, pp. 336-347.

Canudas de Wit, C., H. Olsson, K. J. Åström, and P. Lischinsky (1995). A new model for control of systems with friction. *IEEE Trans. Autom. Control*, **vol. 40**, pp. 419-425.

Tan, Y. and I. Kanellakopoulos (1999). Adaptive nonlinear friction compensation with parametric uncertainties. *Proceedings of the 1999 American Control Conference*, San Diego, CA, pp. 2511-2515.

Bose, B.K., (1986). *Power Electronics and AC Drives.* Englewood Cliffs, NJ: Prentice Hall.

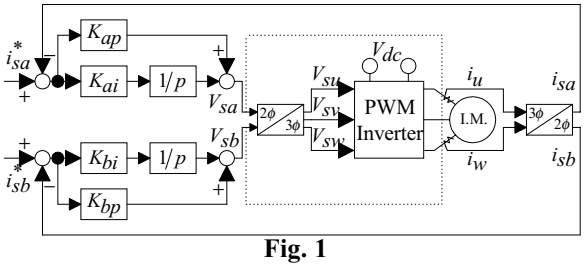

Fig. 1

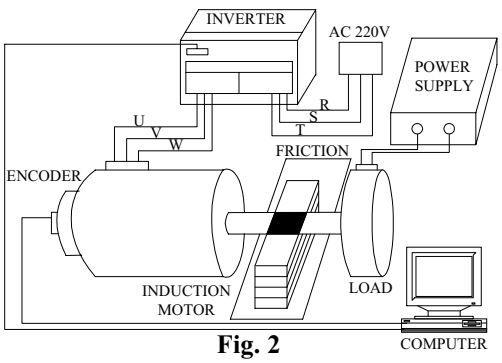

Fig. 2

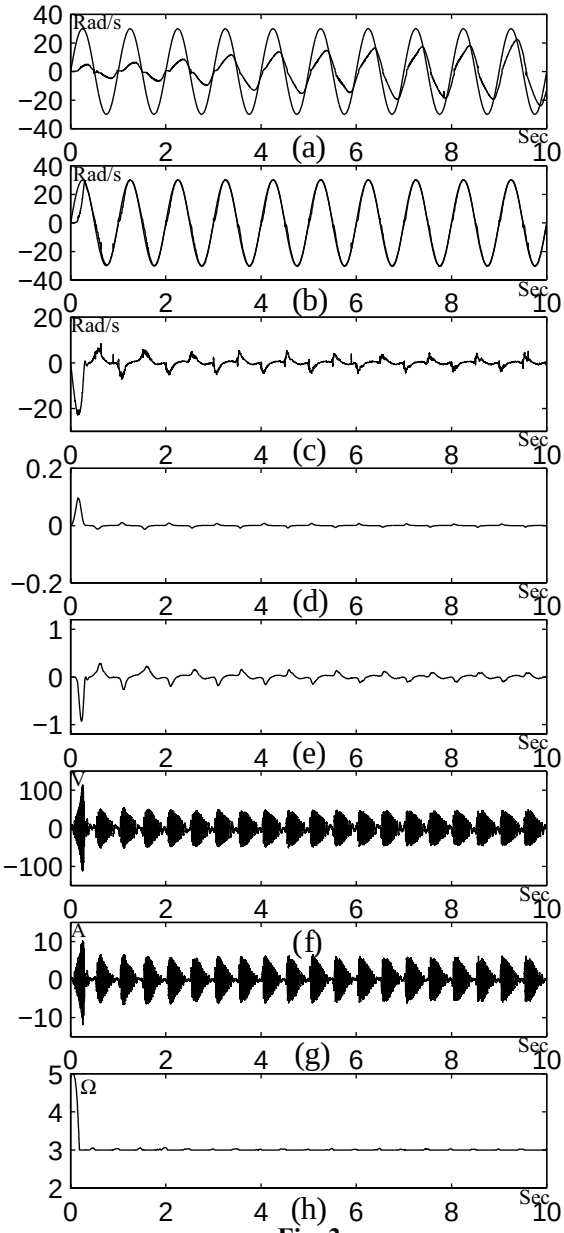

Fig. 3

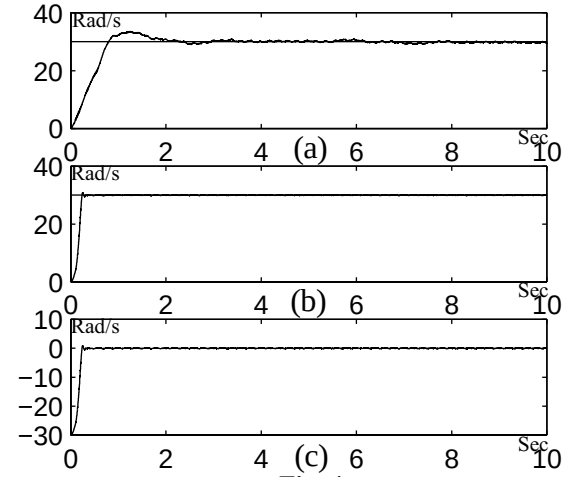

Fig. 4